13th International Brick and
Block Masonry Conference
Amsterdam, July 4-7, 2004

NUMERICAL SIMULATION OF MASONRY UNDER COMBINED LATERAL LOADING AND COMPRESSION

T. Vassilev[1], W. Jäger[2], T. Pflücke[3]

Abstract

The main objective of the contribution is to present a numerical technique designed for the simulation of vertically loaded masonry walls subject to complementary uniaxial bending. The analysis system is based on the discrete modelling of a wall slice of unit length and the formulation of equilibrium conditions in the deformed state, while taking into account the specific material properties. The linearization of the governing differential equation and its piecewise integration in terms of initial parameters lead to a nonlinear transfer matrix formulation. The numerical implementation of the iterative analysis procedure is straightforward and does not require sophisticated software or extensive programming effort. Sample results illustrate the efficiency of the developed approach and its applicability to problems of practical interest.

Key Words

Simulation of masonry, Lateral loading, Vertical loading, Transfer matrix

1 Introduction

The paper addresses the issue of the modelling and analysis of masonry walls under compression combined with uniaxial bending. This aspect of structural behaviour is representative of masonry walls subject to the simultaneous action of vertical and lateral loading like basement walls under earth pressure or external walls under wind load. The interaction of vertically loaded walls with other structural members, like floor slabs for instance, typically also induces combined compression and bending even in the absence of lateral loads.

The theoretical basis of the system solution is provided by a nonlinear formulation of the Transfer Matrix Method. A comprehensive description if its fundamentals can be found among others in Kersten (1962) or Pestel and Leckie (1963). This method was largely elaborated in the nineteen-sixties but has remained since then more or less out of the focus of the wide professional interest. In the shade of the Finite Element

[1] Doz. Dr.-Ing. Todor Vassilev, Dresden University of Technology
[2] Prof. Dr.-Ing. Wolfram Jäger, Dresden University of Technology
[3] Dipl.-Ing. Torsten Pflücke, Dresden University of Technology
Lehrstuhl.Tragwerksplanung@mailbox.tu-dresden.de

Method it quasi moved into oblivion, presumably due to the fact that transfer matrices do not possess the potential and versatility of the finite elements. Numerical solutions with the Transfer Matrix Method can nevertheless be most efficient, whenever, like in the present case, the analysis is based on the linear topology of one-dimensional models and the structural response is governed by a (piecewise-) linear differential equation.

The method has been recently adapted and applied to the buckling analysis of masonry walls (Vassilev et al 2002). This preliminary research focused primarily on the simulation of the material behaviour and the verification of the adopted nonlinear stress-strain relationship. The modelling of the system however was subject to many restrictions with regards to the loading conditions. It was limited exclusively to the simple symmetric case of compression of equal magnitude and eccentricity at the top and bottom edge. The present contribution presents the enhancement of the adopted approach and its extension to related problems of the structural behaviour of masonry under combined compression and bending.

2 Discrete system model

The analysis of the behaviour of structural members under combined vertical and lateral loading is commonly based on the model displayed on Figure 1. If both system parameters – bending stiffness (*B*) and compressive force (*P*) – can be assumed to remain constant under service loading, then there exists a mathematical formulation of the equilibrium which is valid for the whole system. The deformed equilibrium state is given in the case of $B = const.$ and $P = const.$ by the familiar linear differential equation

$$Bw'''' + Pw'' = q \qquad (1)$$

B constant bending stiffness
P constant compressive force
w lateral deflection
q lateral load function

This differential equation possesses a closed-form solution when the lateral load too remains constant along the wall height. For arbitrary loading eq. (1) might have or not have an explicit solution depending on the function $q = q(x)$ of the lateral load.

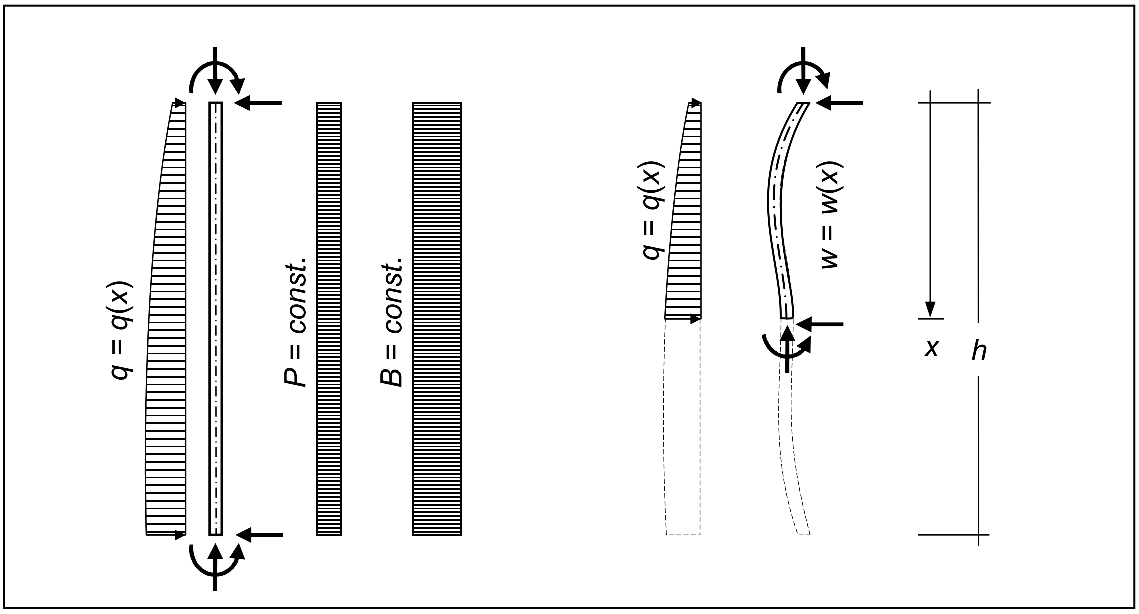

Figure 1 Analysis model for systems with constant parameters

In the case of masonry, however, the mathematical formulation of the equilibrium and the availability of an explicit solution are not subject to the load function alone. A very distinguishing feature of masonry is the dependence of its bending stiffness on the current stress state. This is due foremost to the nonlinear behaviour of the material in compression and its negligible strength in tension. The bending stiffness cannot be expressed as the product of material modulus times moment of inertia. It is also load-dependent and can hence be assumed to remain invariant over the height only in the initial state prior to loading. Under acting loads the bending stiffness will vary due to the nonlinear stress field and as a result of the system modification when cracking in tension occurs. The compressive force too will generally not be constant unless the action of the dead weight is considered to be negligible. The state-dependent bending stiffness and the variable compressive force render the relation (1) inapplicable for masonry and lead to more complex and nonlinear mathematical formulations in the deformed equilibrium state, which generally do not possess explicit solutions.

The approach described in the next section manages to bypass the above handicap by introducing a discrete model and resorting to a linearization of the system parameters. The continuous system is replaced by a discrete and piecewise linear assembly as shown on Figure 2. The analysis model is thus reduced to a set of small segments (*s*) with finite length (h_s). Average approximates of the bending stiffness are evaluated and assumed to be constant within each segment ($B_s = const.$). The variable compressive force and the, in general, arbitrary lateral load are replaced in analogy by a piecewise constant distribution over the height ($P_s = const.$, $q_s = const.$). The accuracy of all the approximates can be arbitrarily steered through variation of the discretisation density.

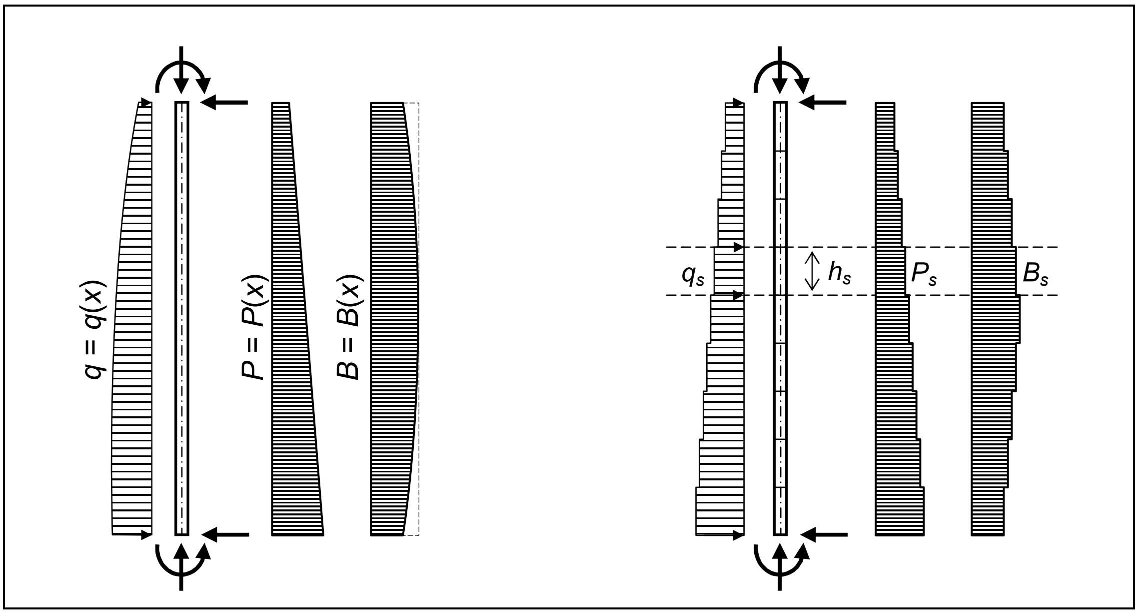

Figure 2 Discrete model for masonry under compression and bending

A relation quasi-identical to eq. (1) can be ultimately derived for the equilibrium in the deformed equilibrium state of the discrete model:

$$B_s w'''' + P_s w'' = q_s \tag{2}$$

B_s bending stiffness of a segment
P_s compressive force within a segment
q_s lateral load on a segment

The similarity of the two differential equations is, however, only formal, for the above relation is not valid for the whole system like eq. (1), but only within the range of each separate segment. The most relevant feature of eq. (2) for the solution procedure described in the following section is the fact that owing to the piecewise linearization of all system parameters – compressive force, lateral load and bending stiffness – it is a linear differential equation with constant parameters and can therefore be explicitly integrated.

3 Transfer matrix procedure

The objectives of the transfer matrix procedure is to determine the state variables in terms of lateral deflection *w*, tangent rotation φ, bending moment *M* and transversal force *V* at each border section (Figure 3), and to establish the overall system response under a specified loading. The procedure comprises four distinct logical steps which have to provide solutions to the following key issues:

(i) to correlate the state variables of two consecutive sections, i.e. the two border sections *s-1* and *s* of an arbitrary segment;
(ii) to establish a functional connection between all segments (s = 1…n), and thus weld the discrete set to a system assembly;
(iii) to determine the state variables (w_0, φ_0, M_0, V_0) of the initial section, i.e. at the top edge of the wall;
(iv) to finally evaluate the state variables all over the wall height and thus provide the overall system response.

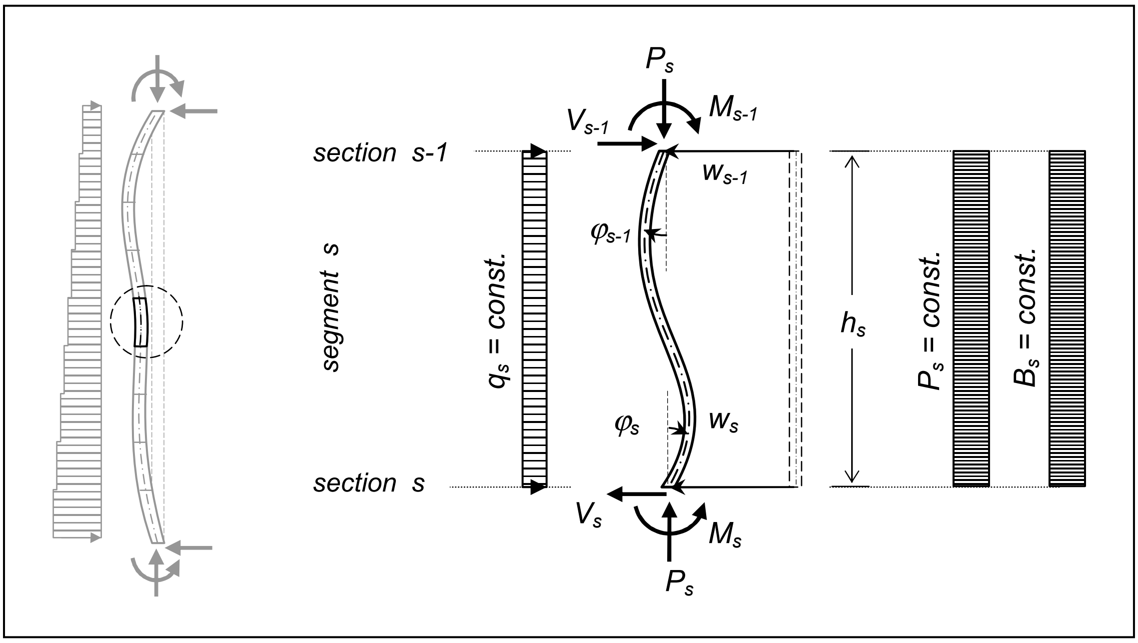

Figure 3 State variables and piecewise constant parameters of a segment

The mathematical basis of the transfer matrix procedure is furnished by the piecewise linear differential equation (2). It denotes the equilibrium conditions in the deformed state of a segment (*s*) under its acting level of compression (P_s = *const.*) and lateral load (q_s = *const.*). It further reflects the internal stress state of the segment in an implicit and generalized form by means of its bending stiffness (B_s = *const.*).

The integration of eq. (2) and its solution in terms of initial parameters within the range of an arbitrary segment lead to the following matrix-vector relation:

$$\mathbf{z_s} = \mathbf{F_s}\,\mathbf{z_{s-1}} \tag{3}$$

z_{s-1}, z_s state vectors at the border sections
F_s field matrix of the segment

The state variables at the respective border sections are arrayed as coefficients of the state vectors:

$$\mathbf{z_s} = \left\{ \begin{array}{c} w_s \\ \varphi_s \\ M_s \\ V_s \\ \hdashline 1 \end{array} \right\} \quad , \quad \mathbf{z_{s-1}} = \left\{ \begin{array}{c} w_{s-1} \\ \varphi_{s-1} \\ M_{s-1} \\ V_{s-1} \\ \hdashline 1 \end{array} \right\} \tag{4}$$

The field matrix has the following concrete structure:

$$\mathbf{F_s} = \left[\begin{array}{cccc:c} 1 & \dfrac{\sin\nu_s}{\nu_s} h_s & -\dfrac{1-\cos\nu_s}{\nu_s^2}\dfrac{h_s^2}{B_s} & -\dfrac{\nu_s - \sin\nu_s}{\nu_s^3}\dfrac{h_s^3}{B_s} & \dfrac{2(1-\cos\nu_s)-\nu_s^2}{2\nu_s^4}\dfrac{q_s h_s^4}{B_s} \\ 0 & \cos\nu_s & -\dfrac{\sin\nu_s}{\nu_s}\dfrac{h_s}{B_s} & -\dfrac{1-\cos\nu_s}{\nu_s^2}\dfrac{h_s^2}{B_s} & \dfrac{\sin\nu_s - \nu_s}{\nu_s^3}\dfrac{q_s h_s^3}{B_s} \\ 0 & \nu_s \sin\nu_s \dfrac{B_s}{h_s} & \cos\nu_s & \dfrac{\sin\nu_s}{\nu_s} h_s & \dfrac{\cos\nu_s - 1}{\nu_s^2} q_s h_s^2 \\ 0 & 0 & 0 & 1 & q_s h_s \\ \hdashline 0 & 0 & 0 & 0 & 1 \end{array} \right] \tag{5}$$

From a purely mathematical point of view its coefficients are a direct outcome of the integration and solution of the non-homogeneous linear differential equation (2). Their physical interpretation is more complex and manifold. Some coefficients incorporate specific features of the segment like its bending resistance and deformability, whereas others reflect kinematical relations or equilibrium conditions. The coefficients in the last column in particular yield the effect of the lateral load applied directly to the segment. The extension by unity of the field matrix and the state vectors is not a deliberate conversion, but rather serves for the specific purpose of the convenient mathematical formulation and implementation in the analysis procedure. It allows in particular to accommodate in a uniform manner the state-dependent as well as the load-dependent coefficients into the body of the field matrix.

All coefficients of the field matrix are functions of the parameter

$$\nu_s = h_s \sqrt{\frac{P_s}{B_s}} \tag{6}$$

It incorporates two essential features of the segment's behaviour in its state of combined compression and bending: on the one hand it reflects the second order effect of the compressive force on the equilibrium, and on the other – the available bending resistance which is a resultant of the current stress and strain state.

The expressions (3) through (6) provide the functional relationship between the state variables of two consecutive sections and give so far the solution of the first key issue. It is evident that the logic of the matrix relation (3) can be extended and applied with the effect to correlate sections which are not necessarily consecutive. The variables of an arbitrary section can in particular be thus defined as functions of the so called system initial parameters, i.e. the state variables of the top edge:

$$\begin{aligned}
\mathbf{z_1} &= \mathbf{F_1}\,\mathbf{z_0} \\
\mathbf{z_2} &= \mathbf{F_2}\,\mathbf{z_1} && = \mathbf{F_2}\,\mathbf{F_1}\,\mathbf{z_0} \\
\mathbf{z_3} &= \mathbf{F_3}\,\mathbf{z_2} && = \mathbf{F_3}\,\mathbf{F_2}\,\mathbf{F_1}\,\mathbf{z_0} \\
&\dots\dots\dots\dots\dots\dots\dots\dots\dots\dots\dots\dots \\
\mathbf{z_s} &= \mathbf{F_s}\,\mathbf{z_{s-1}} && = \mathbf{F_s}\,\mathbf{F_{s-1}}\,\mathbf{...}\,\mathbf{F_2}\,\mathbf{F_1}\,\mathbf{z_0}
\end{aligned} \tag{7}$$

The fusion of the discrete set of segments to a complete assembly is thereupon a trivial matter of matrix multiplication and takes the shape of the product of all the field matrices. It eventually yields an expression similar to (3), which, however, stands for the overall system rather than for a single segment:

$$\mathbf{z_n} = \mathbf{F_n}\,\mathbf{F_{n-1}}\,\mathbf{...F_s}\,\mathbf{F_{s-1}}\mathbf{...F_2}\,\mathbf{F_1} = \mathbf{F}\,\mathbf{z_0} \tag{8}$$

wherein $\mathbf{z_0}$ and $\mathbf{z_n}$ are the state vectors of the top resp. bottom edge, while **F** denotes the system transfer matrix, i.e. of the assembly as a whole. It maps in a generalised form the structural behaviour of the system. The significance of its separate blocks is schematically given below:

$$\mathbf{F} = \begin{bmatrix} f_{11} & f_{12} & f_{13} & f_{14} & f_{1q} \\ 0 & f_{22} & f_{23} & f_{24} & f_{1q} \\ 0 & f_{32} & f_{33} & f_{34} & f_{1q} \\ 0 & 0 & 0 & f_{44} & f_{1q} \\ 0 & 0 & 0 & 0 & 1 \end{bmatrix}$$

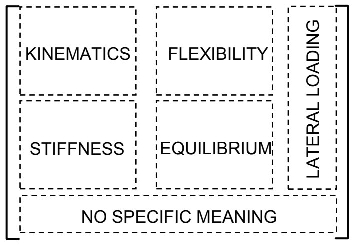

Figure 4 System transfer matrix – structure and physical interpretation

The last open issue thus remains the evaluation of the initial parameters. Unknown are actually only the tangent rotation (φ_0) and the transversal force (V_0), whereas the deflection (w_0) at the top edge is nil and the bending moment (M_0) has a definite value, usually expressed as the product of load (P_0) times eccentricity (e_0):

$$w_0 = 0, \qquad M_0 = P_0\, e_0 \tag{9.1}$$

The matrix relation (8) and the analogical boundary conditions at the bottom edge –

$$w_n = 0, \qquad M_n = P_n\, e_n \tag{9.2}$$

finally lead to a pair of conditional equations, whose solution provides the values of the tangent rotation and transversal force of the top edge:

$$\begin{bmatrix} f_{12} & f_{14} \\ f_{32} & f_{34} \end{bmatrix} \begin{Bmatrix} \varphi_0 \\ V_0 \end{Bmatrix} + \begin{Bmatrix} f_{1q} + f_{13}\, P_0\, e_0 \\ f_{3q} + f_{33}\, P_0\, e_0 - P_n\, e_n \end{Bmatrix} = 0 \tag{10}$$

All the key issues specified in the beginning have so far been given their respective solution and the logical sequence of the transfer matrix procedure can be summarised in conclusion as follows:

(i) compose the field matrices of all segments by means of expression (5);

(ii) evaluate the system transfer matrix as aggregate product according to eq. (8);

(iii) determine the two unknown initial parameters by solving eq. (10);

(iv) evaluate the state variables at each section using the scheme given by eq. (7), and then the resulting value of the curvature

$$\kappa_s = M_s / B_s \tag{11}$$

The final outcome of the above sequence will be the overall system response in terms of internal forces and deformed state. The lateral deflections and bending moments serve in addition as indicators of the overall system stability. This particular aspect of the behaviour gains in relevance with rising wall slenderness and load eccentricity. Decelerated convergence and numeric phenomena like oscillating or rapidly increasing values are the typical forerunners of an unstable state.

4 About the iterative analysis scheme

The Transfer Matrix Solution is only one of the steps belonging to the iterative analysis. The system response it provides is based on an estimate of the bending stiffness. As a result of the nonlinear behaviour of the material in compression and its cracking in tension, the assumed bending stiffness will be subject to change with the ultimate effect of a redistribution of stresses. The analysis requires an iterative approach which is presented schematically on Figure 5 and includes two more essential steps:

- **Section Solution**: evaluation of strains and stresses of all sections; checks on cracking-in-tension and crushing; integration of stresses to stress resultants.
- **Parameters Update**: evaluation and update of the bending stiffness of all segments; update of the effective width in case of cracking.

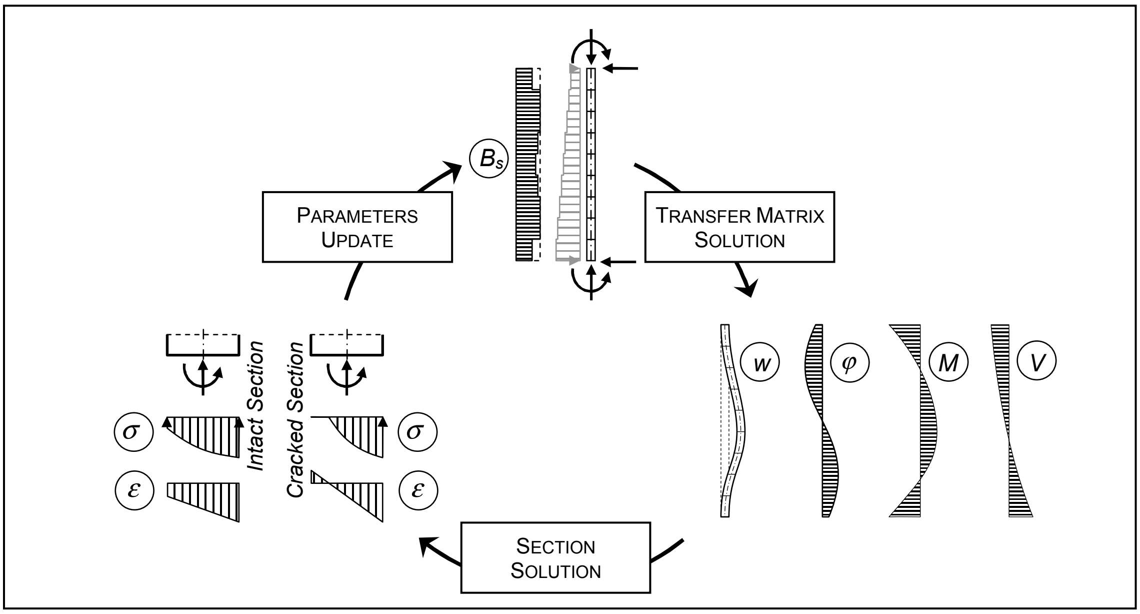

Figure 5 Iterative analysis scheme

The issues related to the evaluation of strains and stresses, integration of the stress resultants and updating of the parameters have been covered in depth and discussed in Vassilev et al (2002). Therefore the details will be intentionally omitted and only the essentials will be outlined below. The underlying material model, in which the state of compression is defined as positive, assumes the following stress-strain function:

$$\sigma(\varepsilon) = \begin{cases} f\left(c\,\dfrac{\varepsilon}{\varepsilon_f} - (c-1)\left(\dfrac{\varepsilon}{\varepsilon_f}\right)^n\right) & (\varepsilon \geq 0) \\ 0 & (\varepsilon < 0) \end{cases} \tag{12}$$

f material strength in compression
ε_f corresponding strain
c, *n* model parameters

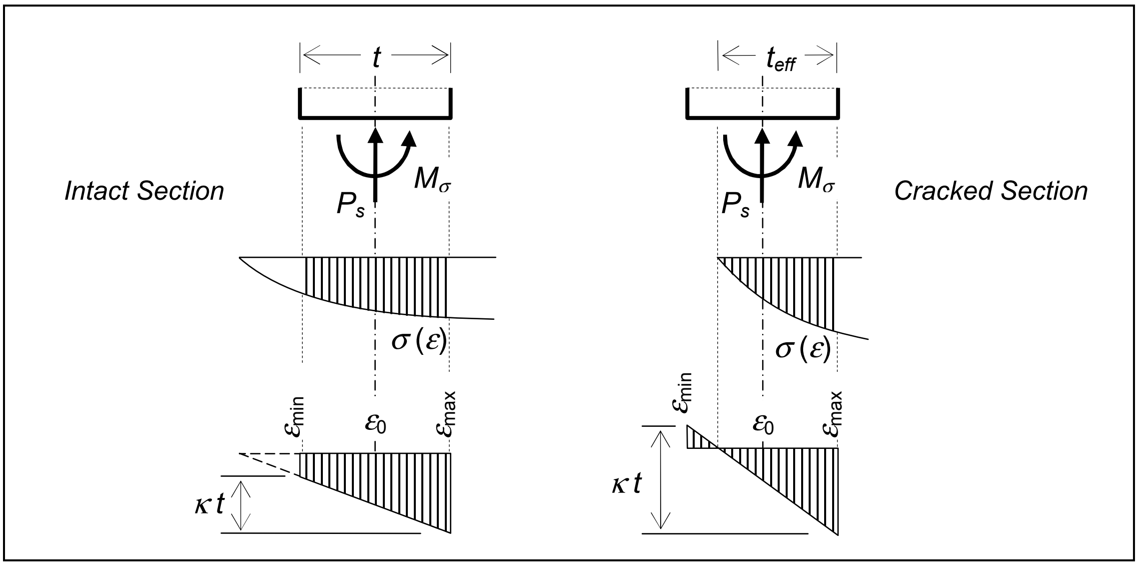

Figure 6 Strain-field and stress distribution at sections

The stress resultant in the section must equal the compressive force in order to satisfy the equilibrium. The conditional equation for a wall slice with unit length reads:

$$\frac{f}{\kappa_s} \int_{\varepsilon_0 - \kappa_s t/2}^{\varepsilon_0 + \kappa_s t/2} \left(c\,\frac{\varepsilon}{\varepsilon_f} - (c-1)\left(\frac{\varepsilon}{\varepsilon_f}\right)^n \right) d\varepsilon = P_s \tag{13}$$

Its solution yields the strain at the centroid (ε_0) and the border strain (ε_{min}, ε_{max}) as displayed in Figure 6. A negative border strain ε_{min} would imply cracking in tension and result in a reduction of the effective width:

$$t_{eff} = \varepsilon_{max} / \kappa_s \tag{14}$$

The stress state can next be determined via the material function (12), and finally the integration of the stresses delivers the updated estimate of the bending stiffness:

$$B_s = \frac{f}{\varepsilon_f\,\kappa_s^3} \int_{\varepsilon_0 - \kappa_s t/2}^{\varepsilon_0 + \kappa_s t/2} \left(c\left(\frac{\varepsilon}{\varepsilon_f}\right)^2 - (c-1)\left(\frac{\varepsilon}{\varepsilon_f}\right)^{n+1} \right) d\varepsilon \; - \; \frac{\varepsilon_0}{\kappa_s^2} P_s \tag{15}$$

The material model above has been specially designed and validated for masonry. Experimental investigations (e.g. Naraine and Sinha 1989, Jäger and Pflücke 2002), disclose a great variety of the behaviour in compression. Depending on the stone-mortar combination, the stress-strain shape may range from quasi linear up to highly nonlinear with features of ductility. The stress-strain function (12) simulates adequately a wide range of real stress-strain relationships. Its explicit integrability is an additional asset which considerably facilitates the implementation and the practical use.

5 Sample results

The investigation of the basement wall on Figure 7 should illustrate the potential of the presented approach. It was analysed within a wide study of the load-carrying capacity of thin layer mortar calcium silicate walls subject to lateral loading (Jäger et al 2003). The $\sigma(\varepsilon)$ function is assumed to be square parabolic. The load action comprises the lateral load (*q*), the vertical load at the top (*P*), the dead weight (*g*) and the reaction (*P* + *gh*). The eccentricity (*e*) at both edges is 1/3 of the wall thickness (*t*). The analysis uses a 20-segment-discretisation. Further data are given in the figure below.

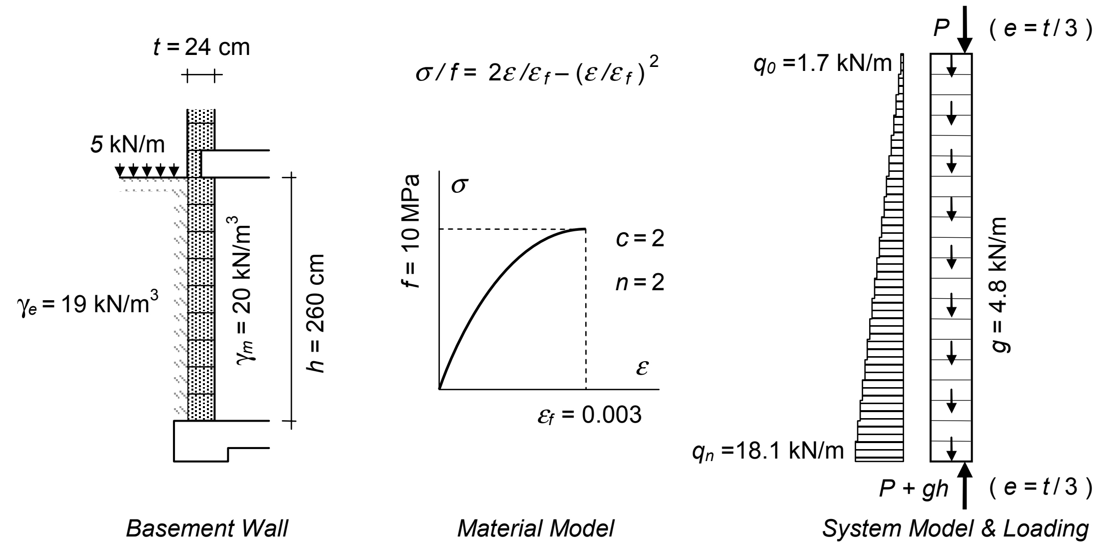

Figure 7 Basement wall under earth pressure and analysis modelling

Two states of ultimate loading are of particular practical interest: the required minimum vertical load at the top (P_{min}) and the maximum load (P_{max}) the wall can bear without failing. Figure 8 presents a partial summary of the results. A rather severe damage due to cracking in tension is common to both cases. The load-bearing performance and the failure mechanisms are however quite different under minimum and maximum load.

The damage pattern on Figure 8a is indicative of an arch thrust under the minimum required vertical load (39 kN). The effect of the lateral load and the dead weight are very tangible at this low level of compression. The effective thickness ratio of the critical section is barely 13%. The maximum stress at its border (σ = 2.8 N/mm^2) is far below the compressive strength (f = 10 N/mm^2), but the cracking in the middle is severe and a further reduction of the vertical load leads to complete failure.

The ultimate state on Figure 8b under the maximum bearable load (566 kN) is a matter of stability. The effect of the lateral load and the dead weight is negligible. The cracking is evenly distributed and affects up to 57% of the wall thickness. The stresses are still lower than *f*, but a further increase of the vertical load leads to instability. The corresponding reduction factor for slenderness and eccentricity is $\Phi = 0.236$.

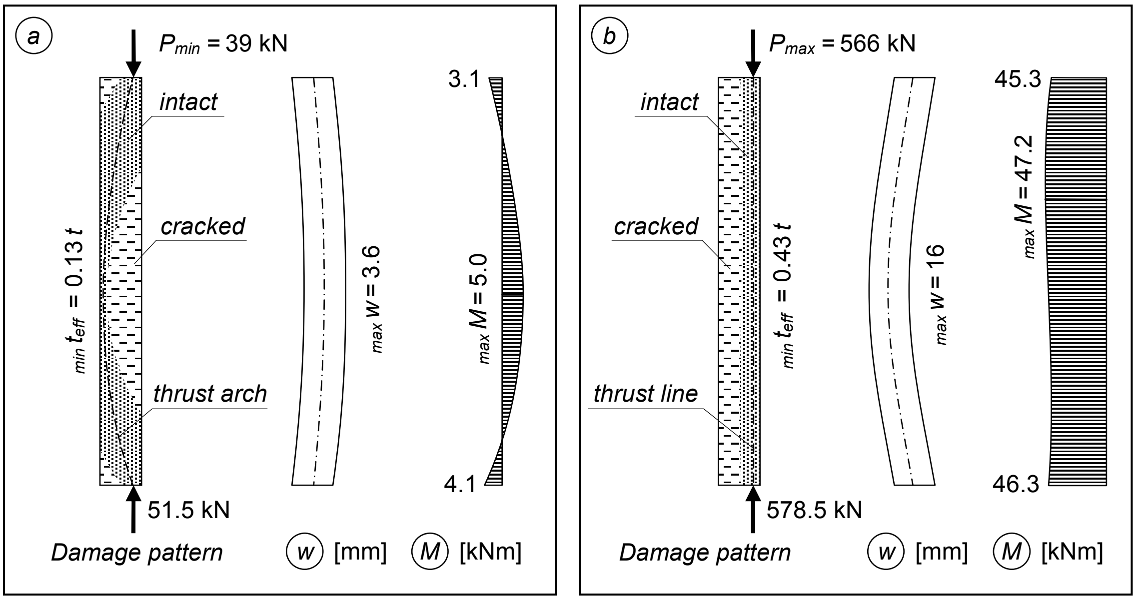

Figure 8 Performance of the basement wall in two ultimate states of vertical loading: (a) under the required minimum load P_{min}; (b) under the highest bearable load P_{max}

Summary

The synergy of the transfer matrix procedure described above and the material model provides an efficient tool for the simulation and analysis of masonry walls subject to combined vertical loading and uniaxial bending. All relevant factors and sources of nonlinearity are taken into account, such as the nonlinear behaviour of masonry, the stress limitation in tension, the system modification under service loading and the second order effects of the deflections on the equilibrium in the deformed state. The approach is applicable to a wide variety of problems of practical interest and provides a reliable basis for the verification of simplified models. The numerical implementation does not require special programming effort but is conveniently based on general purpose software like calculation worksheets.

References

Jäger, W., Pflücke, T. (2002). Untersuchungen zur Knicksicherheit von Mauerwerksbauteilen mit Berücksichtigung großer Exzentrizitäten und nichtlinearer Spannungs-Dehnungs-Beziehungen. Forschungsbericht im Auftrag des DIBt Berlin, TU Dresden, Germany

Jäger, W., Vassilev, T., Pflücke, T., Thieme, M., Baier, G. (2003). Tragfähigkeit von horizontalbeanspruchten Kellerwänden aus Kalksandsteinen unter Verwendung von Dünnbettmörtel. Forschungsbericht im Auftrag des Bundesverbands KS e.V. Hannover, TU Dresden, Germany

Kersten, R. (1962). Das Reduktionsverfahren der Baustatik. Springer Verlag

Naraine, K., Sinha, S. N. (1989), Loading and unloading stress-strain curves for brick masonry. J. Struct. Engrg., ASCE, 115(10), 7631–7644

Pestel, E., Leckie, F.A. (1963). Matrix Methods in Elastomechanics. McGraw Hill

Vassilev, T., Jäger, W., Pflücke, T. (2002). Nonlinear transfer matrix model for the assessment of masonry buckling behaviour. Proc. 6th IMC, London, UK, 512-517